Anomalous chain diffusion in polymer nanocomposites for varying polymer-filler interaction strengths

Monojoy Goswami* and Bobby G. Sumpter†
Computational Chemical Sciences, Oak Ridge National Laboratory, Oak Ridge, Tennessee 37831, USA
(Received 6 October 2009; revised manuscript received 17 December 2009; published 6 April 2010)

Anomalous diffusion of polymer chains in a polymer nanocomposite melt is investigated for different polymer-nanoparticle interaction strengths using stochastic molecular dynamics simulations. For spherical nanoparticles dispersed in a polymer matrix the results indicate that the chain motion exhibits three distinct regions of diffusion, the Rouse-like motion, an intermediate subdiffusive regime followed by a normal Fickian diffusion. The motion of the chain end monomers shows a scaling that can be attributed to the formation of strong "networklike" structures, which have been seen in a variety of polymer nanocomposite systems. Irrespective of the polymer-particle interaction strengths, these three regimes seem to be present with small deviations. Further investigation on dynamic structure factor shows that the deviations simply exist due to the presence of strong enthalpic interactions between the monomers with the nanoparticles, albeit preserving the anomaly in the chain diffusion. The time-temperature superposition principle is also tested for this system and shows a striking resemblance with systems near glass transition and biological systems with molecular crowding. The universality class of the problem can be enormously important in understanding materials with strong affinity to form either a glass, a gel or networklike structures.

DOI: 10.1103/PhysRevE.81.041801 PACS number(s): 82.35.Np, 66.30.Pa, 36.20.Ey, 61.25.hp

I. INTRODUCTION

Anomalous diffusion is an ubiquitous phenomenon in spatially heterogeneous complex systems and has been observed in polymer melts [1–6], granular materials [7], supercooled fluids near glass transition [8–11], colloidal and liquid crystals [12,13], and protein transport in intracellular environments [14]. The slow dynamics in these class of materials, commonly known as soft matter, changes the viscoelastic, electrical, and optical properties of these materials. The slow dynamics leads to a strongly correlated macromolecular transport below a critical temperature [15] thereby pushing the system out of equilibrium, which leads to aging. As the standard statistical mechanics approach is no longer helpful in understanding these out-of-equilibrium systems, it is of no surprise that from a theoretical standpoint, soft matter systems are understood even less than, say, equilibrium glass-forming liquids [16]. Therefore, it is imperative to study these systems using atomistic simulations for a detailed understanding at the molecular level. For this purpose, a polymer nanocomposite (PNC) is a particularly good system to investigate.

In polymer melts, anomalous chain diffusion is an established fact [2,17–19]. In polymer melts, the motion of the chains are entirely different than normal fluids due to the topological constraints present within their macromolecular structures [1,2,19]. Unlike simple fluids, entangled macromolecular motions are constrained by the strong bonds between monomers of the polymer chains. The short and long time dynamics of these entangled polymer chains have been studied extensively with atomistic simulations in polymer melts as well as polymer/solid interfaces [20–24]. Even short chains relax with a number of normal modes, however, superposition in these modes can slow down the motion of the chains as the flexible polymer chains behave as a random-walk like structure [20,22,25]. This slow motion leads to anomalous diffusion of the polymer chains in dense melts. In all cases, the mean square displacement (MSD), $\langle |r_i(t) - r_i(0)|^2 \rangle \propto t^{\alpha}$ where $r_i(t)$ is the monomer position at time t, follows the power law with an exponent α. For Rouse-like motion, $\alpha = 0.5$, which crosses over to the normal Fickian diffusion with $\alpha = 1.0$. The chain motion in the Rouse regime can generally be considered a part of the anomalous diffusion. However, for polymer melts and PNC systems, α for the anomalous diffusion regime falls between 0.5 to 1.0 [26]. For a PNC, in addition to the above constraints, extra complications arise due to the presence of nanoparticles (NPs) that can interact strongly and collectively with the polymer chains. These collective entropic and enthalpic constraints result in profound modifications of the chain relaxation depending on the NP volume fraction, NP size, temperature of the system, chain molecular weight, and NP dispersion [27–29]. The stronger these constraints are, the more difficult it becomes for the chains to move freely, resulting in a non-Einstein decrease in rheological properties and changes in glass transition temperatures [30–32].

Recently, x-ray photon correlation spectroscopy (XPCS) measurements were used to investigate the sub(super)-diffusive behavior of NPs in a PNC melt [33–37]. For polystyrene grafted gold nanoparticles in a polystyrene matrix, it was experimentally shown that relaxation dynamics can be enhanced or reduced depending on the grafting density, NP size, concentration of the grafting chain, and their degree of polymerization [27,38]. Additionally, there has been a large number of molecular dynamics (MD), Monte Carlo (MC) and hydrodynamic studies of PNCs that examined the equilibrium structure, NP diffusion and rheological properties of the system [39–41]. However, most of those studies did not

*goswamim@ornl.gov
†sumpterbg@ornl.gov

directly address the importance of polymer chain motion, and those that did, overwhelmingly investigated normal diffusion of the chain center of mass with a short time Rouse-like behavior [42]. Certainly, these studies give a clear understanding of normal (Fickian) chain diffusion in the presence of a filler but it remains unclear what exactly happens at the intermediate time scales. Should the chains exhibit anomalous diffusion at intermediate time scales as is observed in polymer melts? Will this be an 'universality class' diffusion applicable to all soft-matter system or is it system specific to PNCs?

To answer these questions, we have investigated a model system of a relatively large PNC system using stochastic molecular dynamics simulation and followed the chain dynamics. In this model, we coarse grain (CG) the all-atom polymer model at the molecular level and consider each bead as a monomeric unit. This CG approach simplifies the simulation and explores configuration space much faster during the course of the stochastic simulation [24,43–46]. We demonstrate the anomalous chain diffusion in a PNC system, exemplified by nonexponential relaxation behavior and non-Fickian diffusion under different entropic and enthalpic conditions. The overall relaxation dynamics and swelling phenomena reveal a striking resemblance to strongly correlated systems near glass transition and biological systems with molecular crowding. This study suggests that a fundamental understanding of the anomalous diffusion behavior of polymer chains in PNCs will be of general importance to other soft matter systems that have a strong affinity to form either a glass, a gel or networklike structures [29,47–50].

II. MODEL AND SIMULATION METHOD

Stochastic MD simulations are carried out to examine a model case of spherical NPs dispersed in a polymer matrix of chain length, $N=64$ and 44 nanoparticles. The initial configuration of the model system is randomly generated with a number density of monomers, $\rho=0.7$ and NP volume fraction, $\phi=1.54\%$. All the monomers in the system have mass m_i and Lennard-Jones diameter, σ. This choice allows the simulation to be less computationally expensive, but still do proper justice in understanding the fundamentals of the PNC system as has been shown in recent works [49,51]. Polymer chains are modeled following the Kremer-Grest bead spring polymer model [1], in which bonded beads are connected by finitely extensible nonlinear elastic (FENE) springs represented by,

$$U_{ij}^{\mathrm{FENE}} = -0.5kR_0^2 \ln\left[1-\left(\frac{r_{ij}}{R_0}\right)^2\right], \tag{1}$$

where $R_0=1.5\sigma$ is a finite extensibility and the spring constant, $k=37.5\varepsilon/\sigma^2$, σ being the monomer diameter. The FENE potential in combination with the (excluded volume) repulsive interaction creates a potential well for the flexible bonds that maintain the topology of the molecules. The energetic interaction between any pair of beads is modeled by a truncated and shifted Lennard-Jones potential given by,

$$U_{ij}^{\mathrm{LJ}} = 4\varepsilon\left[\left(\frac{\sigma}{r_{ij}}\right)^{12} - \left(\frac{\sigma}{r_{ij}}\right)^{6} + 1\right], \tag{2}$$

where and r_{ij} is the distance between two particles and ε is the energy parameters for three different interactions described below. Each particle of the system interacts via a short-range repulsive potential whose interaction strength, $\varepsilon \approx \varepsilon_R = 1.0$. U^{LJ} is shifted and truncated with a short range cutoff distance, $r_{ij}^{\mathrm{R}} \leq 2^{1/6}\sigma$. In addition to this repulsive interactions, the NPs and NP-monomer attract each other with interaction strengths, ε_{nn} and ε_{pc}, respectively. The repulsive cutoff is used in conjunction with the attractive cutoffs for the NP-NP interactions and NP-monomer interactions with a cut-off distance, $r_{ij}^{\mathrm{attractive}} \leq 2.5\sigma$. As our focus is to observe the chain dynamics in variety of polymer matrices with a given type of NP, the polymer-NP interaction strength ε_{pc}, has been varied. The above choice of interaction parameters reduce the complex problem of many interactions to a simpler problem with a one variable interaction parameter. The motions of the particles are governed by the classical Newton-Langevin equation,

$$m_i \frac{d\vec{v}_i}{dt} = -\vec{\nabla}U_i - \Gamma\frac{d\vec{r}_i}{dt} + \vec{W}_i(t), \tag{3}$$

where U_i is the net potential energy experienced by particle i and m_i is its mass. Γ is the friction coefficient between the chain monomer and background solvent. $\vec{W}_i(t)$ represents a Gaussian "white noise" with zero mean acting on each particle [52]. The last two terms couple the system to a heat-bath where the "friction term" acts as a heat sink and the "noise term" acts as a heat source. The first advantage of this scheme is that the natural MD integration time steps are larger, thereby permitting simulation on longer time scales. A second advantage comes from the fact that on this time scale, only the mean effect of the stochastic forces acting on the system needs to be considered, leading to the first order temperature relaxation law, which in turn reduces the need of an external thermostat. The dimensionless units are defined as follows, $t^\star = t/\sqrt{m_i\sigma^2/\varepsilon_R}$, $\rho^\star = \rho\sigma^3$, $T^\star = k_BT/\varepsilon$, $U^\star = U/k_BT$ and $r^* = r/\sigma$.

III. RESULTS

All simulations are carried out in the canonical ensemble (NVT) in a cubic box of length, $L=16\sigma$. Periodic boundary conditions (PBC) are used where the image of the central simulation cell (L) is repeated in all the three directions in such a way that if a polymer chain goes outside the box, it reappears from the opposite side of the box with the same velocity. This allows one to simulate an infinite system by modeling a unit cell of volume L^3. The simulations were run for 150×10^6 time steps to achieve equilibrium. After equilibration the data were collected for 50×10^6 time steps with a reasonable size time step, $\Delta t^* = 0.01\tau$. It is important to note that the CG dynamics does not correspond to the real dynamics and a scaling of the CG units is required in order to quantitatively compare results from CG simulations with the experimental data [24,43,44,46]. Although, this needs a sys-

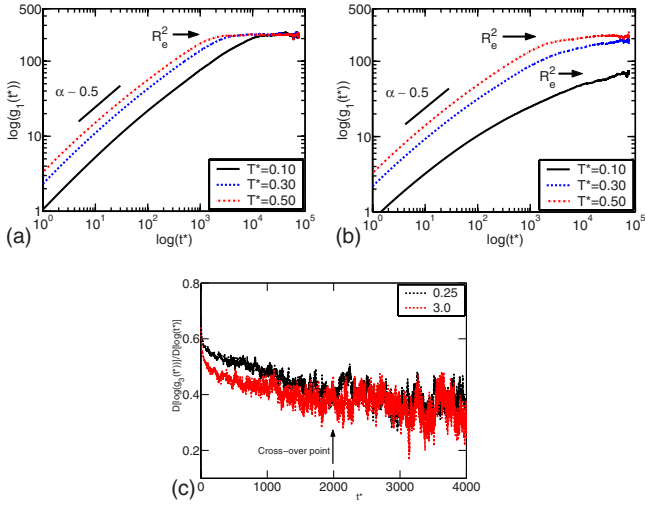

FIG. 1. (Color online) Mean square displacement of the end monomers with respect to the chain center-of-mass (CM) for (a) $\varepsilon_{pc}=0.25$, (b) $\varepsilon_{pc}=2.5$. Black solid line is for $T^*=0.1$, blue dotted line is for $T^*=0.3$ and red dot-dash line is for $T^*=0.5$. R_e^2 represents end-to-end distance square which is also the plateau value of $g_1(t)$ at equilibrium. The power law exponent $\alpha=0.5$ represents Rouse behavior which continues to a longer time-scale than a random walk chain. (c) For $\varepsilon_{pc}=0.25$ (top dashed line) and 3.0 (bottom dashed line), the derivative (referred as D) of log of the end monomers MSD, $g_3(t^*)$ is plotted at a fairly high temperature, $T^*=0.45$. Cross-over time is used to estimate entanglement length by assuming it to be the Rouse relaxation time of a subchain of length N_e. $g_3(t^*)$ is discussed in detail in Fig. 3.

tematic derivation from the chemistry, to get a realistic feeling from the experimental perspective an *ad hoc* time step may be introduced: If Δt^* were converted to real units, it will imply $\Delta t=22\times10^{-15}$ sec for a non-bonding interaction between -CH_2- monomers, given that $\varepsilon_R=0.4742$ kJ/mol and $\sigma=0.428$ nm.

As these studies deal with the diffusion of the chains in a PNC, the structural properties and NP motion is beyond the scope of this paper and can be found in Ref. [49]. Here, we focus on the behavior of the MSD of the chains for three different cases [1]. In the first case, we define the motion of the end monomers with respect to the chain center-of-mass (CM), $g_1(t)=\langle|[r^i_{\rm end}(t)-r_{\rm cm}(t)]-[r^i_{\rm end}(0)-r_{\rm cm}(0)]|^2\rangle$. The second case considers the motion of the CM of the chain, $g_2(t)=\langle|r_{\rm cm}(t)-r_{\rm cm}(0)|^2\rangle$. Third, we consider the motion of the end monomers only, $g_3(t)=\langle|r^i_{\rm end}(t)-r^i_{\rm end}(0)|^2\rangle$. In Fig. 1, $g_1(t)$ is shown for strong and weak interaction parameters, ε_{pc} and three different temperatures, T^*. In Fig. 1(a), the end monomer displacements with respect to the chain CM saturate near to the end-to-end distance of the chain, R_e^2 for all the T^*. $g_1(t)$ shows a Rouse-like (slope=0.5) behavior prior to saturating to their respective squared end-to-end distances (R_e^2), which are as much as an order of magnitude higher than the corresponding radius of gyration, $R_g^2(\approx18)$, of an ideal chain of length 64. In Fig. 1(b), $g_1(t)$ is shown for $\varepsilon_{pc}=2.5$. At this strong ε_{pc}, $g_1(t)$ displays Rouse-like behavior followed by a plateau value near R_e^2. For the Rouse model, the largest relaxation time of a random walk chain is, $\tau_N=\Gamma N R_e^2/3\pi^2 k_B T$, where Γ is the friction coefficient with the viscous background. The largest nondimensionalized relaxation time, $\tau_N^*=\tau_N/\sqrt{m\sigma^2/\varepsilon_R}$ is around 1700 at $T^*=0.1$ for random walk chain of length 64. At $T^*=0.3$ and $T^*=0.5$, τ_N^* is around 1150 and 700, respectively, for random walk chains of length 64. In this simulation, the $t^{0.5}$ behavior can be observed even at considerably longer time scales except at the lowest temperature, $T^*=0.1$. This increase in structural relaxation time may be due to the strong confinement induced by the NPs that causes the chains to take a longer time to reach the saturation limit. The plateauing effect of $g_1(t)$ at R_e^2 is well established in polymer melts [2]. It was quite interesting to see the same behavior of the end monomers with respect to the chain CM is preserved even in the presence of 1.54% NPs, however, at much longer time scale.

Figure 1(c) gives examples of obtaining a rough estimate of the chain entanglement length. The entanglement length is estimated from the cross-over time between the Rouse regime and the reptation regime. The Rouse time is represented by [25,53], $\tau_R=N^2/3\pi^2 W$, where $W=\frac{k_BT}{\zeta b^2}$, ζ being the effective monomer friction and b is the statistical segment length. The prefactor in τ_R relies on the assumptions that the Rouse model is valid for short time scales and the segmental motion occurs on a Gaussian tube [see Doi and Edwards, [53] for details]. A tentative approximation of τ_R is obtained from the derivative of $\log[g_3(t)]$, shown in Fig. 1(c) [54]. Here derivatives of log of the MSD are displayed for two different ε_{pc} at a fairly high temperature. As the long time data is not necessary to estimate the cross-over point, only 4000 time steps are plotted in Fig. 1(c). The maximum of the $\tau_R\approx2000\tau$ for the chain length $N=64$. From the slope of Rouse regime, $\alpha=0.5$, we evaluate $W=0.04$ for a monomer diameter $b=1.12\sigma$. Using the expression for τ_R shown above, this approximately results to a maximum value of $N_e=49$ as the entanglement length. It is important to note that an accurate evaluation of N_e requires the calculation of inner monomer relaxation time. However, due to the unavailability of inner monomer data, we have used end monomer τ_R, which suffer strongly from the contour length fluctuations. The contour length fluctuation makes the relaxation time shorter than that predicted by the original reptation theory. Although this is a point of concern, for the estimation of the "largest" N_e, a crude approximation of the "longest" relaxation time using the end monomers may suffice the purpose of the discussion. It is interesting to note that although the chain length is small, it is higher than the estimated largest entanglement length, i.e., $N>N_e$. The end monomers move faster compared to the central segments of the chains and the MSD of end monomers with respect to the chain CM reaches a plateau value of R_e^2 [55]. In any case, these results do not provide any conclusive evidence of the entanglement of polymer chains in a PNC melt system. However, it highlights the fact that entanglement in a PNC system differs substantially than the entanglement in a simple polymer melt. To study the broad range of transition regime from Rouse-like to reptationlike, larger chain lengths in the presence of nanoparticles must be considered.

This change in relaxation time, with respect to a simple polymer melt, has been observed in other PNC systems too. There have been several experiments for athermal mixtures

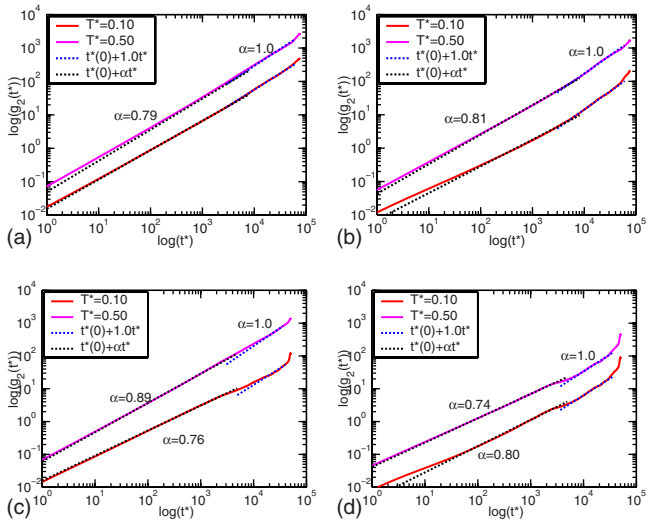

FIG. 2. (Color online) Mean square displacement of chain center of mass for (a) low $\varepsilon_{pc}=0.25$ and (b) high $\varepsilon_{pc}=3.0$. Red solid line (bottom line) represents $T^*=0.1$ and magenta solid line (top line) represents $T^*=0.5$. The black dotted lines are power law fits to t^{α} in a log-log scale for shorter times, where α varies between 0.79–0.81 in this time range. The blue dotted lines (far end of the lines) are long time fits to the power law where the exponent $\alpha=1.0$ indicating a crossover to simple Fickian diffusion. (c) and (d), slopes for larger particles, 2σ, are shown for $\varepsilon_{pc}=0.25$ and 3.0. Note the difference in slopes for the anomalous region.

of thiol terminated polystyrene (PS) chain grafted gold nanoparticles and PS showing increase or decrease in relaxation times with a strong dependence on nanoparticle concentration, nanoparticle size, grafting density, and grafting PS chain degree of polymerization [27,38,56]. For low degree of polymerization of the grafted PS, relaxation time has been found to increase [27]. This may be attributed to the enhancement of τ_N^* for bare nanoparticles. In any case, the bare nanoparticles used in this simulation cannot be directly compared with the grafted NPs, however, the low grafted chain degree of polymerization allows strong interpenetration by the polymer chains of the melt which enthalpically resembles as increase in interactions (ε_{pc}) between the chain and NP represented by ε_{pc}. Overall, this confirms that the confinement effect due to the presence of the NPs may alter the time scale of the Rouse behavior, but not alter the scaling law. Also, at high ε_{pc} and lower temperatures, $g_1(t)$ takes longer to saturate and approach close to R_e^2. For low temperatures and high ε_{pc}, the strong enthalpic confinement may be responsible for the slow motion of the end monomers.

In Fig. 2, $g_2(t)$ for the MSD of the chain CM is shown for $\varepsilon_{pc}=0.25$, and $\varepsilon_{pc}=3.0$ at a fairly high temperature, $T^*=0.5$. For all ε_{pc}, at intermediate time scales, the chain CM MSD follows a power law between $t^{0.79}$ to $t^{0.81}$. At longer times the chain CM diffusion becomes simple Fickian with a power law t^1. The power law fits are shown in black dotted lines at the intermediate time scales and blue dotted lines at longer time scales. Although, the data are not well fitted at short time scales, it has been left out intentionally to give an idea of the gradual increase of slopes from 0.5 to the anomalous diffusion regime. The calculation of MSD at very long times generate poor statistics because of small number of correlation points. Therefore, for very long time scales seen in the end upward movements of the MSD, we do not fit the data. It is worth noting that these MSD data are taken after the simulation was run for 150 million time-steps to equilibrate. The absence of the Rouse-like behavior in these plots therefore does not reflect its absence in the short time motion, i.e., within the first 150 million time steps. In polymer melts the scaling exponents have been found to vary approximately between 0.6–0.8 [1,2]. The present study on PNC melts show that the scaling exponents lie in the upper range of these values. This can be attributed to the fact that in the PNC system, in addition to the highly entangled polymer chains, drag can be caused by the presence of strong interfacial interactions between the NPs and the polymer chains. The overall motion of the polymer chains is affected by the enthalpic interactions between the NPs and the monomers. In an earlier study Salaniwal *et al.* [42]. had shown that for weak interaction strengths, the dynamics of the chains go from short-time Rouse-like motion to normal diffusion at long times. For stronger ε_{pc} their work shows that MSD follows the behavior of some supercooled liquids at temperatures below the onset of caging. In the present study, ε_{pc} is much weaker than that of Salaniwal *et al.* [42], we show that there exists an intermediate time-scale where the chain CM exhibits anomalous diffusion consistent with the results obtained in the simple polymer melts [1,3]. Although the system studied here is simple enough to provide feedback on the exact nature of larger macromolecular systems or stronger polymer-filler interaction strengths, it can very well be used to understand the fundamental physics behind more complex systems. For example, the anomalous scaling exponent was found to be between 0.75–0.86 for biological macromolecules [14] with no substantial temperature dependence for diffusion of tracer proteins in highly concentrated random-coil polymer and globular protein solutions. In a set of MD simulations, Neusius *et al.* [57] have found the scaling between 0.3–0.7 for a different class of biological macromolecules, namely oligopeptide chains in aqueous solutions. Our results for PNC melts have nearly the same range of power law exponents for different polymer-NP interaction strengths, although the density is much higher and the chain lengths are shorter compared to the earlier experimental and simulation studies referred above. The higher density in the PNC system may cause higher drag, which in turn reduces the motion of shorter chains and hence the PNC system shows a close resemblance with the exponent values of "tracer protein" diffusion.

Figures 2(c) and 2(d) compares the results of the motion of larger particles for the same monomer number density ($\rho=0.7$) with a diameter 2σ, i.e., particles that are twice the size used in this simulation. Results for two temperatures $T^*=0.1$ and $T^*=0.5$ are shown for weak and strong interaction strengths, $\varepsilon_{pc}=0.25$ and $\varepsilon_{pc}=3.0$, respectively. As can be seen from these two plots, chain motion follows the same behavior as the smaller particles, anomalous diffusion followed by Fickian diffusion. In these cases, the anomalous diffusion can be seen to prevail for longer time scale. A noticeable feature of these plots is the different slopes for different temperatures and interaction strengths which may

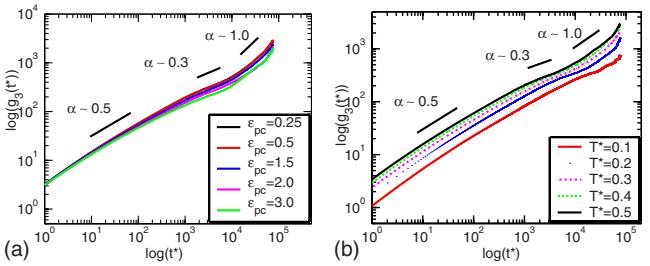

FIG. 3. (Color online) Comparison of the mean square displacements of the end monomers, $g_3(t)$, at different temperature and ε_{pc}. (a) $g_3(t)$ is plotted for different ε_{pc} at $T^*=0.45$. Black, red, blue, magenta and green solid lines (from left to right) represent $\varepsilon_{pc}=0.25$, 0.5, 1.0, 1.5, 2.0 and 3.0 respectively. (b) Different lines represent different temperatures, red solid line: $T^*=0.1$, blue dotted line: $T^*=0.2$, magenta dot-dash line: $T^*=0.3$, green dotted line: $T^*=0.4$ and black solid line: $T^*=0.5$ (right to left in grayscale). In both the plots, the three short black solid lines are to guide the eye to their respective slopes.

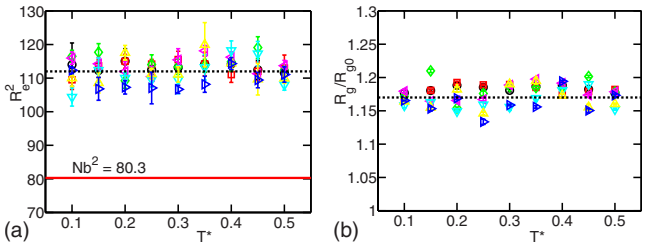

FIG. 4. (Color online) (a) End-to-end distance square, $\langle R_e^2\rangle$ and (b) ratio of the radius of gyration of the chain $\langle R_g\rangle$ and radius of gyration of random walk chain, $\langle R_{g0}\rangle$ as a function of temperature for different polymer-NP interaction strengths. Black circles $\varepsilon_{pc}=0.25$, red square, $\varepsilon_{pc}=0.5$, green diamond, $\varepsilon_{pc}=1.0$, magenta left-triangle $\varepsilon_{pc}=1.5$, light blue down-triangle $\varepsilon_{pc}=2.0$, yellow up-triangle $\varepsilon_{pc}=2.5$, and blue right-triangle $\varepsilon_{pc}=3.0$. The red solid line in (a) shows the ideal chain $\langle R_e^2\rangle$ of chain length 64. In the presence of NPs, around 40% swelling is observed compared to the ideal chain of length $N=64$ and $b=1.12\sigma$. The black dashed line in (b) shows an average $\langle R_g\rangle/\langle R_{g0}\rangle=1.17$ which is in reasonable agreement with the experimental results by Tuteja *et al.* [29].

be attributed to the depletion interaction [58] between the polymer chain and the nanoparticle that has also been observed in many biological systems [59–61]. As T^* increases, an increase in slopes is observed for weaker interaction strengths, $\varepsilon_{pc}=0.25$, however, it reverses for higher interaction strengths, $\varepsilon_{pc}=3.0$. The overall behavior can be explained as follows: As entropy increases, the system breaks down for lower enthalpic state, $\varepsilon_{pc}=0.25$, leading to faster diffusive motion and hence an increase in the exponent. However, for higher enthalpic state, $\varepsilon_{pc}=3.0$, the formation of strong networks [47–49,62,63] even at high temperature, $T^*=0.5$, leads to a sluggish motion of the chains thereby causing a decrease in the slope.

In Fig. 3, we show $g_3(t)$ for different ε_{pc} and T^*. Figure 3(a) is plotted for a higher temperature, $T^*=0.45$ to represent the variation with ε_{pc}. The choice of high T^* ensures the presence of an entropically disordered state which may not be affected by the equilibrium of the chain end monomers. In both Figs. 3(a) and 3(b), $g_3(t)$ shows Rouse-like behavior at short times, up to 10^3 time steps. It then crosses over to a $t^{0.3}$ scaling before reaching simple Fickian diffusion for all the ε_{pc}. The change in ε_{pc} causes a small change in the subdiffusive behavior, albeit keeping the exponent, $\alpha\sim 0.3$ for all the cases. In Fig. 3(b), $g_3(t)$ is shown for different temperatures at the lowest ε_{pc} value. All the temperatures show a similar scaling, except at $T^*=0.1$. Irrespective of system temperature and polymer-NP interaction strengths, $g_3(t)$ shows an intermediate regime of anomalous diffusion between a Rouse-like behavior and long time Fickian diffusion. For $T^*=0.1$ (red solid line), lower entropy may be obstructing the MSD to go beyond the anomalous diffusion regime within the time frame of the simulation. At even longer times it is possible that the low entropy curve would follow normal diffusion.

In Fig. 4, the average end-to-end distance square, $\langle R_e^2\rangle$ and ratio of the radius of gyration of the chain with the ideal chain, $\langle R_g\rangle/\langle R_{g0}\rangle$, where $\langle R_{g0}\rangle$ is the radius of gyration of an ideal chain, are shown. In Fig. 4(a), $\langle R_e^2\rangle$ is plotted as a function of temperature for different ε_{pc} and compared with the ideal chain theoretical value. For an ideal chain of chain length $N=64$ and the effective monomer size $b=1.12\sigma$, $\langle R_e^2\rangle=80.3$ and $\langle R_g^2\rangle=13.4$, respectively. For different ε_{pc} and T^*, the calculated $\langle R_e^2\rangle$ are plotted in Fig. 4(a). It can be seen that $\langle R_e^2\rangle$ fall within 10% of their median value for all the ε_{pc}. Although there are variations at different ε_{pc} values, there is no distinguishing feature for what the dependence of $\langle R_e^2\rangle$ could be with respect to the set of ε_{pc} studied. However, it should be noted that for all the ε_{pc}, the chains swell with around 40% increase in $\langle R_e^2\rangle$.

Next, we calculated $\langle R_g\rangle/\langle R_{g0}\rangle$, shown in Fig. 4(b), to investigate the observed swelling effect more critically. For all the temperatures, $\langle R_g\rangle/\langle R_{g0}\rangle$ has a mean 1.17 which is remarkably close to the experimentally observed value by Tuteja *et al.* [29], although there are differences in the NP volume fraction and polymer-NP interactions between the experiment and simulation. In the experimental work, the swelling behavior was attributed to the much larger increase in polymer dimension due to the *solid* solvent behavior of the nanoparticles as opposed to any nanoparticles behaving as 'a good' solvent which can cause normal swelling of the chains. From a thermodynamics point of view, the previous experiment along with this simulation entirely explains the swelling phenomena. From a dynamics standpoint, swelling leads to a sluggish movement of the chains and this contributes to the sub-diffusive motion of the chains. The swelling of the chains and its effect on sub-diffusive motion has also been observed in hydrogels as drug-delivery systems where the drugs released through polymer matrices follow a non-Fickian diffusion [64–66]. In the swelled PNC system, the stresses arising during the polymer swelling process have significant effects on the transport of the chains thereby causing hindrance to the normal diffusion of the chains.

To better understand the anomalous behavior it is imperative to examine the structural relaxation at different length scales, $S(q,t)=\frac{1}{N}\Sigma_i \exp[i\vec{q}\cdot\vec{r}_i(t)]$ where, $\vec{q}$ is the wave vector defined by, $|\vec{q}|=2\pi/\ell$. Calculations were performed for long and short wavelengths (ℓ) i.e., $q\sigma=1.5$ and $q\sigma=0.3$, starting

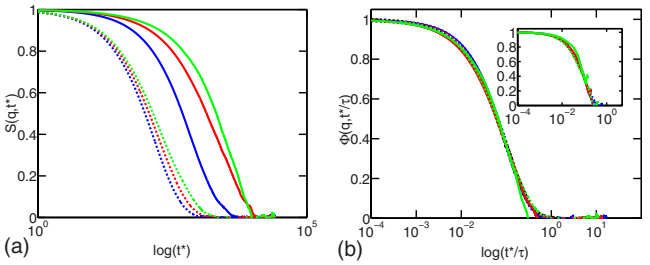

FIG. 5. (Color online) Structural relaxation time as a function of time. For all the plots, all solid lines signify $T^*=0.1$ and dashed lines signify $T^*=0.45$. The blue, red and green colors (left to right) represent $\varepsilon_{pc}=0.25$, $\varepsilon_{pc}=1.5$ and $\varepsilon_{pc}=3.0$ respectively. (a) $S(q,t^*)$ for $q\sigma=1.5$ for the two temperatures and for low, intermediate and high polymer-NP interaction strengths. (b) Master curves using time-temperature superposition principle, $\Phi(q,t^*)$ plotted as a function of $\log(t^*/\tau)$ at small wavelength, $q\sigma=1.5$. All the curves fit quite well with a 'single' stretched exponential of the form, $\exp(-(t^*/\tau)^{0.8})$. Inset plot is for long wavelength, $q\sigma=0.3$.

with the first peak of the static structure factor $S(q)$ and extending to longer length scales. In Fig. 5(a), $S(q\sigma=1.5,t^*)$ is plotted at $T^*=0.1$ and 0.45 for three ε_{pc} values. In case of normal Fickian diffusion, relaxation follows simple exponential behavior, $S(q,t^*)\sim\exp(-t/\tau)$. It can be seen that for all T^* and ε_{pc}, $S(q,t^*)$ decays slower than exponential. This slow relaxation dynamics is not only specific to the anomalous diffusion of the polymer chains in PNC melts, it has been observed in supercooled polymer melts near glass transition [19], colloidal systems [67], liquid crystals [12], disordered media [68], and hydrated proteins [14]. For all these cases, the nonexponential behavior is associated with a non-Markovian aging process. Other features of Fig. 5(a) come from the energy considerations, as T^* increases, entropy of the chains causes the structure factors to decay faster. As ε_{pc} increases, enthalpy of the system is strong enough to enhance a networklike "caging" effect which in turn slows down the decay of $S(q,t^*)$. To understand the PNC system in a broader perspective, we interpret the structural relaxation data in the light of mode coupling theory (MCT). The time-temperature superposition (TTSP) principle states that all $S(q,t^*)$ at the same q but different temperatures should coincide, if time is properly scaled, $\Phi(q,t^*/\tau)=S(q,t^*/\tau_q)$. Here, the time scaling factor τ_q is chosen as the relaxation time of the chain CM at a given q. In Fig. 5(b), TTSP plots of the dynamic structure factor are shown for different temperatures and ε_{pc}. As can be seen, all the curves fall on a master curve suggesting that the TTSP *does* work for this PNC system at the shorter length scales. We also fit the TTSP master curve with a stretched exponential at this $q\sigma$ value. It was observed that $S(q=1.5,t^*/\tau)$ fits extremely well with the function $\exp[-(t^*/\tau_q)^\beta]$ where the exponent is, $\beta=0.8$. For polymer melts near glass transition [3], it has been observed that the small length scale motions are well described by the MCT, which surprisingly, is found to be true in the present case, although the system is nowhere near the glass transition temperature. This may be attributed to the formation of a "strong network" or as discussed earlier, the "onset of clustering transition." The stretched exponential decay appears to be universal in nature and akin to the behavior of strongly correlated systems. Inset of Fig. 5(b) shows $\Phi(q,t^*/\tau)$ for longer length scales, i.e., for $q\sigma=0.3$. For intermediate length scales (not shown here), the TTSP fails considerably, however, for longer length scales the curves fall on the top of each other except at lower temperatures and higher ε_{pc} values. These deviations can be explained if we consider $S(q,t^*)$ decay consists of a *fast* Markovian process and a *slow* non-Markovian process [69]. The separation of $S(q,t^*)$ can be written as, $S(q,t^*)=S_T(q,t^*)+S_N(q,t^*)$, where S_T is the "fast decay" due to thermal fluctuations and S_N is the slower part resulting from the "enthalpic caging" of the chains in networklike structures [49]. Thus the anomalous diffusion of the chains is inherently dependent on the nature of interactions between monomers and NPs.

IV. CONCLUSION

In conclusion, our results overwhelmingly support the presence of three distinct regions of chain motion: a Rouselike motion, an anomalous diffusion at intermediate timescales, followed by a Fickian diffusion at longer time scales. The MSD is found to follow an exponent α between 0.5–1.0 and a non-exponential decay in structural relaxation is observed. Strong interactions between the NPs and monomers cause the chains to relax slowly compared to their polymer melt counterpart. Interestingly it is observed that the entanglement length is smaller than the chain length. Although, the results are not conclusive enough as it represents only a small system, it can well be highlighted that entanglement in the presence of nanoparticles requires a completely different meaning for which larger systems need to be studied. The behavior of the chain relaxation belongs to an universality class, Kohlraush-Williams-Watts (KWW) stretched exponential decay, and can also be seen in polymer melts and other dense complex fluids near the glass transition [3,13,70]. Deviation from normal diffusion occurs in several transport processes [71] near glass transition, in the present study though, the system under investigation is far from glass transition. The observed anomalous diffusion behavior is the result of "a different kind of transition," which was previously referred to as the onset of clustering [49,72].

From the results of this study, the anomalous diffusion of polymer chains in a PNC system is established to be the part of an "universality class" transport phenomena. The origin of the anomalous diffusion stems from the slow relaxation dynamics of the polymer chains and is fundamentally due to the presence of strong entropic and enthalpic interactions between the monomers and NPs. At small length scales, MCT can describe the chain relaxation extremely well, however, for longer length the reduction in chain relaxation is due to the presence of strong long-range attractions. The relaxation time is not only specific to this system, it can be applied to systems with larger NPs or longer chain lengths as was investigated in earlier experiments [27]. The range in temperature and interaction strengths falls within a cluster transition temperature regime where the overall dynamics of the chains slows down. In the presence of NPs, polymer chains swell giving rise to 1.17 times increase in the radius of gyration compared to the ideal chain of the same length and a 40%

increase in end-to-end distance squared. These results are in very good agreement with recent experimental findings [29]. Although some of the earlier experimental studies [28,73] did not show any change in polymer chain radius of gyration, we strongly believe, if the NPs dispersion is homogeneous, the swelling could be observed easily.

Overall, these results reflect an universal class of transition akin to the glass transition in supercooled systems. As such, the fundamental results of the diffusive behavior of polymer chains in PNCs provided herein should be of considerable use in understanding the controlled formation of nanostructures, designing high performance materials and to improve our knowledge of transport of proteins in intracellular medium. Finally, the universal nature of polymer chain diffusion in PNCs observed in this study will be important for the quest of a unified theory of molecular motions in strongly correlated systems.

ACKNOWLEDGMENTS

This work was supported by the Division of Materials Science and Engineering (DMSE), U.S. Department of Energy (DoE), Office of Basic Energy Sciences (BES) under Contract No. DEAC05-00OR22725 with UT-Battelle, LLC at Oak Ridge National Laboratory (ORNL).

[1] K. Kremer and G. S. Grest, J. Chem. Phys. **92**, 5057 (1990).
[2] W. Paul, Chem. Phys. **284**, 59 (2002).
[3] K. Binder, C. Bennemann, J. Baschnagel, and W. Paul, Lecture Notes in Physics **519**, 124 (1999).
[4] H. Popova and A. Milchev, Phys. Rev. E **77**, 041906 (2008).
[5] J. L. A. Dubbeldam, A. Milchev, V. G. Rostiashvili, and T. A. Vilgis, EPL **79**, 18002 (2007).
[6] A. Milchev and K. Kremer, Europhys. Lett. **26**, 671 (1994).
[7] A. S. Keys, A. R. Abate, S. C. Glotzer, and D. J. Durian, Nat. Phys. **3**, 260 (2007).
[8] W. K. Kegel and A. van Blaaderen, Science **287**, 290 (2000).
[9] S. Sastry, Nature **409**, 164 (2001).
[10] S. P. Das, Rev. Mod. Phys. **76**, 785 (2004).
[11] E. R. Weeks, J. C. Crocker, A. C. Levitt, A. Schofield, and D. A. Weitz, Science **287**, 627 (2000).
[12] L. De Gaetani, G. Prampolini, and A. Tani, J. Chem. Phys. **128**, 194501 (2008).
[13] L. De Gaetani, G. Prampolini, and A. Tani, J. Phys. Chem. B **111**, 7473 (2007).
[14] D. S. Banks and C. Fradin, Biophys. J. **89**, 2960 (2005).
[15] R. Klages, G. Radons, and I. M. Sokolov, *Anomalous Transport: Foundations and Applications* (Wiley-VCH, Berlin, 2008).
[16] L. E. Cugliandolo, in *Slow Relaxations and Nonequilibrium Dynamics in Condensed Matter*, edited by J.-L. Barrat, M. Feigelman, J. Kurchan, and J. Dalibard (Springer, Berlin, 2003), p. 367.
[17] K. Binder, A. Milchev, and J. Baschnagel, Annu. Rev. Mater. Res. **26**, 107 (1996).
[18] J. Baschnagel and K. Binder, Macromolecules **28**, 6808 (1995).
[19] C. Bennemann, C. Donati, J. Baschnagel, and S. C. Glotzer, Nature (London) **399**, 246 (1999).
[20] V. A. Harmandaris, V. G. Mavrantzas, D. N. Theodorou, M. Kroger, J. Ramirez, H. C. Ottinger, and D. Vlassopoulos, Macromolecules **36**, 1376 (2003).
[21] V. A. Harmandaris and K. Kremer, Macromolecules **42**, 791 (2009).
[22] J. T. Padding and W. J. Briels, J. Chem. Phys. **117**, 925 (2002).
[23] V. A. Harmandaris, K. C. Daoulas, and V. G. Mavrantzas, Macromolecules **38**, 5796 (2005).
[24] V. A. Harmandaris and K. Kremer, Soft Matter **5**, 3920 (2009).
[25] P. G. de Gennes, *Scaling Concepts in Polymer Physics* (Cornell University Press, Ithaca, NY, 1979).
[26] T. McLeish, in *Theoretical Challenges in the Dynamics of Complex Fluids*, edited by Tom McLeash (Kluwer Academic Press, Boston, 1997), Vol. 339.
[27] H. Oh and P. F. Green, Nature Mater. **8**, 139 (2009).
[28] S. Sen, Y. Xie, S. K. Kumar, H. Yang, A. Bansal, D. L. Ho, L. Hall, J. B. Hooper, and K. S. Schweizer, Phys. Rev. Lett. **98**, 128302 (2007).
[29] A. Tuteja, P. M. Duxbury, and M. E. Mackay, Phys. Rev. Lett. **100**, 077801 (2008).
[30] M. E. Mackay, T. T. Dao, A. Tuteja, D. L. Ho, B. van Horn, H.-C. Kim, and C. J. Hawker, Nature Mater. **2**, 762 (2003).
[31] P. Rittigstein, R. D. Priestly, L. J. Broadbelt, and J. M. Torkelson, Nature Mater. **6**, 278 (2007).
[32] A. Bansal, H. Yang, C. Li, K. Cho, B. C. Benicewicz, S. K. Kumar, and L. S. Schadler, Nature Mater. **4**, 693 (2005).
[33] H. Guo, G. Bourret, M. K. Corbierre, S. Rucareanu, R. B. Lennox, K. Laaziri, L. Piche, M. Sutton, J. L. Harden, and R. L. Leheny, Phys. Rev. Lett. **102**, 075702 (2009).
[34] S. Srivastava, A. K. Kandar, J. K. Basu, M. K. Mukhopadhyay, L. B. Lurio, S. Narayanan, and S. K. Sinha, Phys. Rev. E **79**, 021408 (2009).
[35] A. K. Kandar, S. Srivastava, J. K. Basu, M. K. Mukhopadhyay, S. Seifert, and S. Narayanan, J. Chem. Phys. **130**, 121102 (2009).
[36] S. Narayanan, D. R. Lee, A. Hagman, X. Li, and J. Wang, Phys. Rev. Lett. **98**, 185506 (2007).
[37] R. Aravinda Narayanan, P. Thiyagarajan, S. Lewis, A. Bansal, L. S. Schadler, and L. B. Lurio, Phys. Rev. Lett. **97**, 075505 (2006).
[38] L. Meli, A. Arceo, and P. F. Green, Soft Matter **5**, 533 (2009).
[39] C. R. Iacovella and S. C. Glotzer, Nano Lett. **9**, 1206 (2009).
[40] G. Allegra, G. Raos, and M. Vacatello, Prog. Polym. Sci. **33**, 683 (2008).
[41] M. Wang and R. J. Hill, Soft Matter **5**, 3940 (2009).
[42] S. Salaniwal, S. K. Kumar, and J. F. Douglas, Phys. Rev. Lett. **89**, 258301 (2002).
[43] S. O. Nielsen, G. Srinivas, and M. L. Klein, J. Chem. Phys. **123**, 124907 (2005).
[44] W. Tschöp, K. Kremer, J. Batoulis, T. Burger, and O. Hahn, Acta Polym. **49**, 61 (1998).

[45] H. Fukunaga, J. Takimoto, and M. Doi, J. Chem. Phys. **116**, 8183 (2002).
[46] D. Fritz, C. R. Herbers, K. Kremer, and N. F. A. van der Vegt, Soft Matter **5**, 4556 (2009).
[47] T. Kashiwagi, F. M. Du, J. F. Douglas, K. I. Winey, R. H. Harris, and J. R. Shields, Nature Mater. **4**, 928 (2005).
[48] A. Tuteja, D. M. Duxbury, and M. E. Mackay, Macromolecules **40**, 9427 (2007).
[49] M. Goswami and B. G. Sumpter, J. Chem. Phys. **130**, 134910 (2009).
[50] J. Hooper and K. Schweizer, Macromolecules **40**, 6998 (2007).
[51] C. D. Knorowski, J. A. Anderson, and A. Travesset, J. Chem. Phys. **128**, 164903 (2008).
[52] W. F. van Gunsteren and H. J. C. Berendsen, Mol. Phys. **45**, 637 (1982).
[53] M. Doi and S. F. Edwards, *The Theory of Polymer Dynamics* (Clarendon Press, Oxford, 1986).
[54] Q. Sun and R. Faller, Macromolecules **39**, 812 (2006).
[55] M. Pütz, K. Kremer, and G. S. Grest, Europhys. Lett. **49**, 735 (2000).
[56] A. Arceo, L. Meli, and P. F. Green, Nano Lett. **8**, 2271 (2008).
[57] T. Neusius, I. Daidone, I. M. Sokolov, and J. C. Smith, Phys. Rev. Lett. **100**, 188103 (2008).
[58] J. Hooper, K. Schweizer, T. Desai, R. Koshy, and P. Keblinski, J. Chem. Phys. **121**, 6986 (2004).
[59] N. Kozer, Y. Y. Kuttner, G. Haran, and G. Schreiber, Biophys. J. **92**, 2139 (2007).
[60] A. N. Semenov, Macromolecules **41**, 2243 (2008).
[61] R. J. Ellis, Trends Biochem. Sci. **26**, 597 (2001).
[62] M. Goswami and B. G. Sumpter, *NANO '08, 8th IEEE Conference on Nanotechnology* (IEEE, Arlington, TX, 2008), p. 748.
[63] A. P. Kumar, D. Depan, N. S. Tomer, and R. P. Singh, Prog. Polym. Sci. **34**, 479 (2009).
[64] A. Prokop, E. Kozlov, G. Carlesso, and J. M. Davidson, Adv. Polym. Sci. **160**, 119 (2002).
[65] F. J. Xu, E. T. Kang, and K. G. Neoh, Biomaterials **27**, 2787 (2006).
[66] N. A. Peppas and R. W. Korsmeyer, *in Hydrogels in Medicine and Pharmacy*, edited by N. A. Peppas (CRC Press, Boca Raton, FL, 1987), Vol. III.
[67] I. Santamaría-Holek, A. Perez-Madrid, and J. M. Rubi, J. Chem. Phys. **120**, 2818 (2004).
[68] J. Bouchaud and A. Georges, Phys. Rep. **195**, 127 (1990).
[69] E. J. Saltzman, G. Yatsenko, and K. S. Schweizer, J. Phys.: Condens. Matter **20**, 244129 (2008).
[70] R. Bandyopadhyay, D. Liang, H. Yardimci, D. A. Sessoms, M. A. Borthwick, S. G. J. Mochrie, J. L. Harden, and R. L. Leheny, Phys. Rev. Lett. **93**, 228302 (2004).
[71] E. W. Montrell and B. J. West, in *Fluctuation Phenomena*, edited by E. W. Montrell and J. L. Lebowitz (North-Holland, Amsterdam, 1987).
[72] S. K. Kumar and J. F. Douglas, Phys. Rev. Lett. **87**, 188301 (2001).
[73] S. Sen, Y. Xie, A. Bansal, H. Yang, K. Cho, L. S. Schadler, and S. K. Kumar, Eur. Phys. J. Spec. Top. **141**, 161 (2007).